Light and nutrient availability affect the size-scaling of growth in phytoplankton

Zhi-Ping Mei [a], Zoe V. Finkel [b], Andrew J. Irwin [a,*]

[a] Department of Mathematics and Computer Science, Mount Allison University, Sackville, NB, Canada E4L 1E6
[b] Environmental Science Program, Mount Allison University, Sackville, NB, Canada E4L 1A5

ARTICLE INFO

ABSTRACT

Communities of marine phytoplankton consist of cells of many different sizes. The size-structure of these communities often varies predictably with environmental conditions in aquatic systems. It has been hypothesized that physiological differences in nutrient and light requirements and acquisition efficiencies contribute to commonly observed correlations between phytoplankton community size structure and resource availability. Using physiological models we assess how light and nutrient availability can alter the relative growth rates of phytoplankton species of different cell sizes. Our models predict a change in the size dependence of growth rate depending on the severity of limitation by light and nutrient availability. Under conditions of growth-saturated resource supply, phytoplankton growth rate ($mol\,C\,cell^{-1}\,time^{-1}$) scales with cell volume with a size-scaling exponent of $\frac{3}{4}$; light limitation reduces the size-scaling exponent to approximately $\frac{2}{3}$, and nutrient limitation decreases the exponent to $\frac{1}{3}$ as a consequence of the size-scaling of resource acquisition. Exponents intermediate between $\frac{1}{3}$ and $\frac{3}{4}$ occur under intermediate availability of light and nutrients and depend on the size-scaling of pigment photoacclimation and the size range examined.

1. Introduction

The size-structure of phytoplankton communities is an important determinant of carbon and nutrient cycling, the pelagic and benthic food web structure, and carbon export to the deep sea (Tremblay et al., 1997; Laws et al., 2000). In general, higher rates of community primary production are associated with increasing abundance of larger cells, increased trophic transfer efficiency, and increased carbon export into the deep sea. Field observations (Chisholm, 1992; Li, 2002; Cermeño et al., 2006) and the fossil record (Finkel et al., 2005, 2007) provide evidence that the size structure of plankton communities are affected by environmental conditions. Modeling biogeochemical responses to climate change requires descriptions of the size structure of phytoplankton communities and the size-scaling of growth and loss processes.

Cell size affects many of the processes that determine growth rates: light harvesting, nutrient uptake and internal metabolic transportation networks (Fig. 1) and many of these rates, M, can be described as power-law functions of organism size, $M = aV^b$, where a is a size-independent constant, V is a measure of organism size, and b is the size-scaling exponent. When resources are limiting, the surface area to volume ratio imposes fundamental constraints on rates of resource acquisition. At low nutrient concentrations, diffusive flux limits nutrient uptake through Fick's law, with a volume-scaling exponent of $\frac{1}{3}$ (Munk and Riley, 1952), while maximum nutrient uptake may be regulated by surface area (Aksnes and Egge, 1991) or independent of surface area (Berg and Purcell, 1977). Under light limitation phytoplankton adjust their chlorophyll content and photosynthetic machinery to maximize growth (Falkowski, 1991; Richardson et al., 1983; MacIntyre et al., 2002). At low irradiance, the geometric cross-section, proportional to volume to the power $\frac{2}{3}$, will regulate the cell's ability to gather light (Finkel et al., 2004). Cell volume constrains the absorptive efficiency of pigment molecules and as a result larger cells tend to have lower intracellular concentrations of chlorophyll a and the size-scaling of light-limited photosynthetic rate scales with cell volume with an exponent closer to $\frac{2}{3}$ than $\frac{3}{4}$ (Finkel, 2001; Finkel et al., 2004; Fujiki and Taguchi, 2002). These size-dependent resource acquisition rates have a dramatic effect on the size structure of the phytoplankton community, restricting the viability of larger cells under low resource conditions (Cermeño et al., 2006; Irwin et al., 2006). Intracellular transportation networks regulate metabolic rate with a $\frac{3}{4}$ exponent on cell size (West et al., 1997; Banavar et al., 2002). The ubiquity of the $\frac{3}{4}$ size-scaling exponent associated with metabolic rates (Kleiber, 1947; Hemmingsen, 1960; Peters, 1983a) may be a consequence of the size-scaling of internal biological transportation networks with fixed delivery

rates at their outer edges (West et al., 1997); if the proportion of mass in the transportation system does not change with cell size, then the maximum transport rate will scale with cell volume with a $\frac{3}{4}$ exponent under resource replete conditions (Banavar et al., 2002). Nutrient uptake, light absorption, and metabolic transportation processes all vary with cell volume, with different size-scaling exponents and in combination with size-selective loss rates in grazing, parasitoid and viral attack, and nutrient recycling will result in variability in the size structure of phytoplankton communities under different environmental conditions (Armstrong, 2003; Raven and Waite, 2004; Irwin et al., 2006).

A fusion of transportation network allometry with the size-dependence of light and nutrient acquisition is essential for developing the next generation of coupled ocean biogeochemical general circulation models incorporating size-structured communities to predict rates of carbon fixation, trophic transfer through the food web, and carbon export to the deep sea. An analysis of the interaction of the biophysical constraints on the size-scaling of phytoplankton growth rate due to light and nutrient acquisition and the cellular transportation network capacity over a range of sub-saturating to saturating photon flux densities and nutrient concentrations is needed. We construct two models with different fundamental assumptions about what ultimately controls growth rate. In the first model the size-dependence of growth is set by the minimum of two processes: growth rate due to nutrient uptake and diffusion, and photosynthesis. In the second model growth rate is controlled by the metabolic transportation network capacity, which can be limited by the supply of energy and materials through nutrient diffusion and photosynthesis.
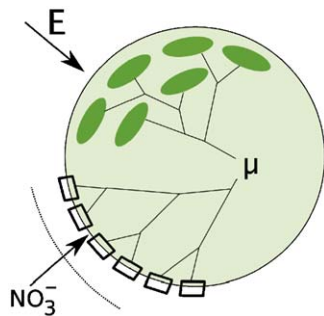

Fig. 1. Schematic illustrating the interaction of size-dependent processes affecting growth rates of phytoplankton. Resources collected by chloroplasts (dark ovals) and nutrient porters (boxes on the cell surface) are processed and the metabolic products transported throughout the cell. All three processes are necessary for balanced growth and each has a different allometry. Environmental conditions and cell size jointly determine the allometric exponent of growth.

2. Model

Our goal is to examine the effect of resource acquisition on the size-scaling of phytoplankton growth over a range of environmental conditions. Phytoplankton growth can be rate limited by light, nutrients, or inherent metabolic rate limitations imposed by intracellular metabolic networks. Each of these impose different size-scaling relationships and their relative importance will depend on resource availability. We formulate two models. (I) A resource acquisition model in which light absorption and nutrient uptake determines growth through saturating functions, with maximum rates determined by their geometric constraints and (II) a metabolic network model in which maximum growth is determined by intracellular metabolic transportation networks, but can be limited by resource availability.

We constrain our models with a fundamental set of observations regarding the size-scaling of phytoplankton growth rates. Under resource saturating conditions, the growth exponent should be $\frac{3}{4}$. Other exponents are possible, e.g., $\frac{2}{3}$, but we will assume the conventional choice supported by the preponderance of empirical evidence (Kleiber, 1947; Hemmingsen, 1960; Dodds et al., 2001). At very low irradiance, the growth exponent should be smaller than $\frac{3}{4}$, possibly $\frac{2}{3}$ because of the geometric cross-section (Eq. (3)) or as small as 0.55 ± 0.05 (Finkel, 2001). When nutrients are extremely scarce and growth is thus limited by diffusion, the growth exponent should be $\frac{1}{3}$ consistent with diffusion limitation of resource uptake (Eq. (8)).

Growth rates are often reported as biomass-normalized rates, but the conversion between cellular and biomass-normalized rates depends on the biomass-volume scaling relationship. In phytoplankton, biomass sometimes scales allometrically with volume, $B \propto V^{3/4}$, because of vacuolation in large cells, especially diatoms and dinoflagellates (Strathmann, 1967; Sicko-Goad et al., 1984; Menden-Deuer and Lessard, 2000). For small cells, the relationship may be close to linear, $B \propto V$, and the relationship may change with taxonomic group (Verity et al., 1992; Raven and Waite, 2004; Irwin et al., 2006). Our models are described using volume rather than biomass because the fundamental processes affecting size-scaling of light absorption and nutrient acquisition depends on a cell's geometric size rather than its biomass. The parameters for size-scaling relationships used in the computations are summarized in Table 1.

2.1. Resource acquisition model

We define phytoplankton growth rate μ (mmol C cell^{-1} d^{-1}) as the minimum of the potential growth rate from irradiance, P (mmol C cell^{-1} d^{-1}), and nutrient uptake, ρ (mmol N cell^{-1} d^{-1}), converted to C units

$$\mu = \min(P, \rho R) \tag{1}$$

Table 1
Parameters for size-scaling relationships used in the models.

Parameter	Symbol	a	Unit	b	Reference
Maximum photosynthesis	P_{max}	1.19×10^{-10}	mmol C cell^{-1} d^{-1}	$\frac{3}{4}$	a,b
Intracellular Chl a concentration	c_i	Eq. (4)	mg chl cell^{-1} μm^{-3}	$-\frac{1}{3}$	b
Maximum NO$_3^-$ uptake	ρ_{max}	5.94×10^{-11}	mmol N cell^{-1} d^{-1}	$\frac{2}{3}$	See text
Half saturation for NO$_3^-$	K_m	0.1	mmol N m^{-3}	$\frac{1}{3}$	c

The intercept corresponds to the value of the parameter at $V = 1 \, \mu m^3$. In the text, the intercept a and slope b have subscripts to identify the scaling relationship, i.e., P_{max}, c_i, ρ_{max}, K_m.
   a Using $\mu_{max} = 2.5 \, d^{-1}$ (Raven et al., 2005) and C quota of 4.75×10^{-11} mmol C cell^{-1} (Finkel et al., 2004).
   b Finkel et al. (2004).
   c Harrison et al. (1996).

where $R = \frac{106}{16}$ is the molar C:N ratio. Phytoplankton growth rate is additionally regulated by the flow of resources and metabolic products within their cellular metabolic networks. Metabolism and cell division are the end result of a multitude of biochemical reactions and biophysical processes, for example nutrient diffusion and uptake, light absorption and electron transport, and the transportation of biosynthetic products throughout the cell (Fig. 1). The delivery of intermediate products to specific locations within the metabolic network may be ultimately responsible for the size-scaling of metabolic rates. The allometry of these metabolic networks is incorporated into the scaling of empirically defined maximum photosynthetic capacity P_{max} (mmol C cell^{-1} d^{-1}) (López-Urrutia et al., 2006).

Cellular photosynthetic rate P (mmol C cell^{-1} d^{-1}) varies with irradiance E (μmol photons m^{-2} d^{-1}):

$$P = P_{max} \tanh\left(\frac{\sigma\phi E}{P_{max}}\right) \tag{2}$$

where the quantum yield of photosynthesis $\phi = 0.06$ mol C (mol photons)$^{-1}$ is independent of cell size (see Fig. 9.11 of Falkowski and Raven, 2007). The absorption cross-section σ (m^2 cell^{-1}) and maximum photosynthetic rate P_{max} are both expressed per cell. The absorption cross-section σ and the intracellular chlorophyll concentration vary with size due to an optical intracellular shading effect referred to as the package effect (Morel and Bricaud, 1981)

$$\sigma = 4\pi r^2 Q(2\sigma_{sol}^* c_i r) \tag{3}$$

where $\sigma_{sol}^* = 0.04$ m^2 (mg chl a)$^{-1}$ is the absorption cross-section of pigment in solution, r (m) is the cell radius, c_i (mg chl a m^{-3}) is the intracellular pigment concentration (discussed below) and $Q(\rho) = 1 + 2e^{-\rho}/\rho + 2(e^{-\rho} - 1)/\rho^2$ is a dimensionless saturating function describing the effects of cell size and c_i on σ. An optimization balancing the synthesis costs against the increased cellular cross-section predicts that intracellular chlorophyll concentration c_i is proportional to $V^{-1/3}$ in agreement with observations (Agustí, 1991), making the magnitude of the package effect independent of cell size, when E is less than the saturating irradiance E_k, and c_i is proportional to $V^{-1/4}$ when $E > E_k$ (Finkel et al., 2004). We express intracellular chlorophyll concentration as a power-law function, $c_i = a_{c_i} V^{b_{c_i}}$ and consider exponents b_{c_i} ranging from $-\frac{1}{3}$ to 0, corresponding to volume-scaling exponents for total cellular chlorophyll from $\frac{2}{3}$ to 1. Intracellular chlorophyll concentration is also regulated by irradiance, generally decreasing with increasing irradiance and described by making a_{c_i} dependent on E

$$a_{c_i} = 4.6 + 21 \exp(-0.008E) \tag{4}$$

The coefficients in this equation are estimated from a regression on intracellular chlorophyll concentrations over irradiances ($E \leq 175\,\mu$mol m^{-2} s^{-1}) and cell volumes ranging from 30 to 300 μm^3 (Finkel et al., 2004). Other photoacclimation strategies include changes in pigment composition and photosynthetic unit structure which could be included in future versions of the model.

Nutrient acquisition is a complex process which we simplify greatly, incorporating the major size-dependent effects: diminished uptake due to diffusion at low resource concentrations and maximum uptake regulated either by surface area or a cell's resource demand. Fortunately, both features can be incorporated into a Michaelis–Menten equation

$$\rho = \frac{\rho_{max} N}{K_m + N} \tag{5}$$

where $\rho_{max} = a_{\rho_{max}} V^{b_{\rho_{max}}}$ (mmol NO$_3^-$ cell^{-1} d^{-1}) is the maximum uptake rate and $K_m = a_{K_m} V^{b_{K_m}}$ (mmol NO$_3^-$ m^{-3}) is the half-saturation constant. One possible choice for the size-scaling of

these parameters is that $\rho_{max} \propto V^{2/3}$ and $K_m \propto V^{1/3}$. Under low nutrient concentrations, $\rho \propto V^{1/3}$, equivalent to diffusion regulation, and under high nutrient concentrations, $\rho \propto V^{2/3}$ as surface area controls maximum uptake (Aksnes and Egge, 1991). The half-saturation constant depends on characteristics of the nutrient porters and the diffusion boundary layer (Pasciak and Gavis, 1974, 1975), so K_m should be a linear combination of terms proportional to cell radius and the radius of a single nutrient porter (Armstrong, 2008, Eq. (9)). Maximum uptake may not be regulated by surface area (Berg and Purcell, 1977) and dynamic quota models sometimes contain variable maximum uptake rates (Grover, 1991) to permit very rapid uptake.

2.2. Metabolic transportation network model

Phytoplankton growth requires the flow of resources through internal networks. This effect arises downstream from resource acquisition; excess resource acquisition cannot reduce this effect except by causing damage or inhibition to the metabolic network. In the resource acquisition model, transportation network allometry is implicitly included in the size-scaling of P_{max}. In the metabolic transportation network model, photosynthetic rate and nutrient uptake are limited by biophysical factors, such as pigment concentration and nutrient diffusion. The size-scaling due to metabolic networks is imposed independent of resource acquisition. If resources limit growth the size-dependence of growth rate will deviate from the 3/4 exponent predicted by metabolic networks. The effects of the metabolic network and resource acquisition can be joined by making cell growth μ (mmol C cell^{-1} d^{-1}) the minimum of three potential growth rates:

$$\mu = \min(M, P, \rho R) \tag{6}$$

determined by maximum metabolic rate, M, potential photosynthetic rate, P, and potential nutrient uptake, ρ, all as cellular rates (mmol C cell^{-1} d^{-1} or mmol N cell^{-1} d^{-1}). Transportation networks predict metabolic rate under resource-saturating conditions to be $M = a_\mu V^{3/4}$ and we set $a_\mu = 1.19 \times 10^{-10}$ mmol C cell^{-1} d^{-1} to match the maximum growth rate from the resource acquisition model (Table 1). The minimum function does not permit co-limitation in which a near limiting supply of one resource imposes a greater demand on another resource. The primary difference and advantage of this model over the resource acquisition model is that there is no need to assign photosynthesis or nutrient uptake as the ultimate constraint on maximum growth rate or need to know the size-scaling of P_{max} or ρ_{max}. As a result, the definition of potential photosynthetic rate is

$$P = E\sigma\phi. \tag{7}$$

Maximum potential nutrient uptake through the cell surface, as limited only by diffusive flux, is

$$\rho = 4\pi D(C_\infty - C_0)r \tag{8}$$

where $D = 1.5 \times 10^{-9}$ m^2 s^{-1} is the diffusion coefficient of NO$_3^-$ in seawater (Pasciak and Gavis, 1974), C_∞ and $C_0 = 0$ mmol m^{-3} are the concentration of nutrients in the bulk seawater and at the cell surface, respectively, and $r \propto V^{1/3}$ is the cell radius. We set $C_0 = 0$ to determine the maximum rate of diffusive flux; cells not limited by nutrients may have a smaller rate of nutrient uptake and $C_0 > 0$.

In variable environments, a variable internal stores (Droop-type) model is usually required (Grover, 1991), but the size-dependence of this approach presents additional complications which we do not consider here. The additional but important mechanisms of size-dependent loss (grazing, sinking) and realistic ocean circulation are outside the scope of this study (Kiørboe, 1993; Armstrong, 2003; Raven and Waite, 2004).

3. Results

3.1. Resource acquisition model

The size-scaling of maximum growth rate, μ_{max} under completely saturating resource conditions is the smaller of P_{max} and ρ_{max} (Eqs. (1), (2), (5), Fig. 2). These relative magnitudes are determined by the intercepts on the size-scaling of maximum photosynthetic rate and nutrient uptake, $a_{P_{max}}$ and $a_{\rho_{max}}$. If $a_{P_{max}} = \frac{106}{16} a_{\rho_{max}}$ then $P_{max} = \rho_{max}$ at $V = 1\ \mu m^3$ and $\mu_{max} = \rho_{max} < P_{max}$ for $V > 1\ \mu m^3$ and therefore nutrient uptake rates will limit growth for cells bigger than $1\ \mu m^3$. The size-scaling exponent for μ_{max} will be $\frac{2}{3}$, matching the size-scaling exponent of maximum nutrient uptake. To ensure growth is limited by photosynthesis for cells below about $10^6\ \mu m^3$ resulting in a size-scaling exponent for μ_{max} of $\frac{3}{4}$, we set $a_{\rho_{max}} = 5.94 \times 10^{-11}$ mmol N cell^{-1} d^{-1} (Table 1). The potential maximum photosynthetic and nutrient uptake rates, with exponents $\frac{3}{4}$ and $\frac{2}{3}$, respectively, are shown in Fig. 2. If a smaller intercept for maximum nutrient uptake rate is used, large cells can be limited by nutrient acquisition even under nutrient saturating conditions; reducing $a_{\rho_{max}}$ reduces the maximum exponent on μ below $\frac{3}{4}$, possibly as low as $\frac{2}{3}$. Models with different size-scaling of saturated nutrient uptake (Berg and Purcell, 1977; Armstrong, 2008) will require similar adjustments to ensure a $\frac{3}{4}$ volume-scaling exponent of maximum growth rate.

Resource limitation leads to complex relationships between growth rate, as limited by photosynthesis or nutrient uptake, and cell volume. In general the relationships are not purely power-law functions, but we approximate them as power-law functions by finding a regression line through $\mu(V)$ sampled uniformly on
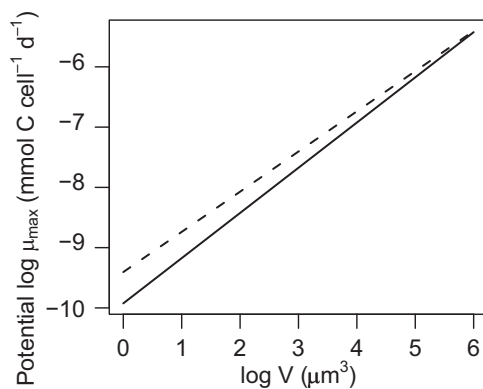

Fig. 2. The allometric relationship of maximum growth rate μ_{max} determined by the minimum of nutrient (ρ_{max}, dashed line) and light (P_{max}, solid line) regulated growth.

$\log(V)$, and summarize these exponents as a function of environmental conditions (E or NO_3^-). These empirical growth size-scaling exponents vary from $\frac{1}{3}$ to $\frac{3}{4}$ (Fig. 3) achieving extreme values at strongly limiting and completely saturating resource conditions. Four cases can be identified: (i) saturating resources, (ii) nutrient concentrations low enough to limit growth of cells of all sizes, and (iii) irradiance low enough to limit growth of cells of all sizes, and (iv) for intermediate resource conditions, a wide range of exponents are achieved as different sized cells have their growth regulated by a combination of these factors. Saturated growth yields an exponent of $\frac{3}{4}$. Under nutrient limiting conditions, diffusion regulates growth and the exponent is $\frac{1}{3}$, determined by the difference between the allometric exponent for ρ_{max} and K_m of NO_3^- uptake (Eq. (5)). Finally, under nutrient saturating and extremely low light conditions, the size-scaling exponent of growth is $\frac{2}{3}$ (Fig. 3a, low E and Fig. 3b, $E = 5$ line). At low irradiance, the size-scaling of the cellular absorption cross-section, σ, dominates the scaling of P (Eq. (2)). The size-scaling of σ is affected by the cellular pigment concentration, the package effect and the geometric cross-section of the cell. The package effect is independent of cell size if the size-scaling exponent of cellular chlorophyll, b_{chl}, is $\frac{2}{3}$, as predicted by an optimization for light-limited cells (Finkel et al., 2004) and data (Agustí, 1991). Using this exponent for cellular chlorophyll, the size-scaling exponent for light-limited growth rate is $\frac{2}{3}$ because of the scaling of the geometric cross-section of the cell (Eq. (3)). Chlorophyll per cell varies with irradiance and cell size (Finkel et al., 2004). Increasing irradiance decreases chlorophyll per cell (represented as intracellular chlorophyll concentration, Eq. (4)). We explored a range of larger exponents for cellular chlorophyll from $\frac{2}{3}$ to 1 and observed a modest increase in the size-scaling exponent of light-limited growth rate from $\frac{2}{3}$ to 0.71 as larger cells were able to acquire more light with the extra pigment (Fig. 4). Increasing the size-scaling exponent of cellular chlorophyll increased P for large cells; the size-scaling exponent of growth varies from the σ-determined $\frac{2}{3}$ to the P_{max}-determined $\frac{3}{4}$, with the exact value of the exponent determined by the degree to which cells of different sizes are limited for light. If pigment has a cost with a significant proportion of the cell's energy budget, we would expect larger cells to be disadvantaged at high values of b_{chl}. In the absence of this cost, large cells will have a large package effect at large b_{chl}; σ and P will both increase with b_{chl}. In our model, the cellular chlorophyll volume-scaling exponent is an independent parameter and there are no metabolic costs for pigment; the resulting decrease in light absorption per mg of chlorophyll is never offset by the cost of pigment synthesis.

The resource acquisition model uses familiar relationships for the size-scaling of photosynthesis and resource acquisition, but there are some undesirable features. The relative maximum
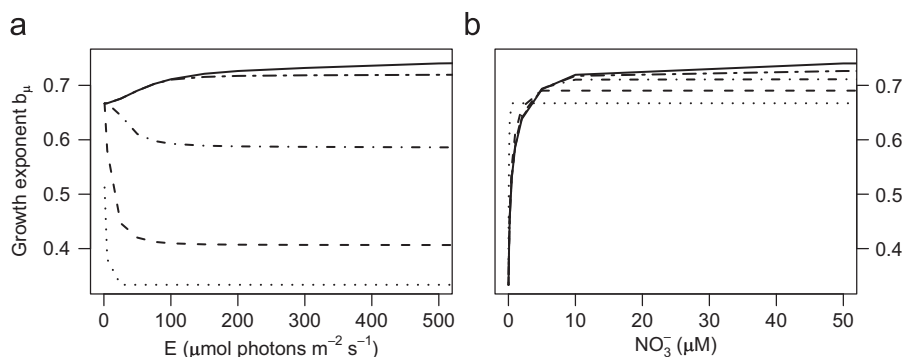

Fig. 3. Size-scaling exponent of growth for the resource acquisition model. (a) b_μ as a function of E for $NO_3^- = 0.01$ (dotted line), 0.1 (dashed), 1 (dash–dotted), 10 (dash-long dash), and 50 μM (solid). (b) b_μ as a function of NO_3^- for $E = 5$ (dotted line), 50 (dashed), 100 (dash–dotted), 200 (dash-long dash), and 500 μmol photons m − 1 (solid). Results are for a size-scaling exponent of $\frac{2}{3}$ for cellular chlorophyll a.

photosynthetic rate and nutrient uptake rate must be finely balanced to ensure the $\frac{3}{4}$ rule for resource saturated growth. Furthermore, this scaling relationship derives from the size-scaling of $P_{\max}$, which likely has little to do with the scaling of photosynthesis, per se, but is a consequence of size-scaling constraints associated with the metabolic transportation network. The choice of intercept on the size-scaling relationship of maximum nutrient uptake rate determines the extent to which the $\frac{2}{3}$ exponent of maximum resource uptake can regulate the allometry of growth under saturating conditions; a large

maximum nutrient uptake rate is required to ensure the $\frac{3}{4}$ size-scaling exponent of resource saturated growth. The metabolic network model avoids these deficiencies.

3.2. Metabolic transportation network model

In the metabolic transportation network model, growth is limited by the minimum of photosynthesis, P, nutrient acquisition, ρ, or by metabolic capacity (M). Cellular resource acquisition rates (Eqs. (7) and (8)) are affected by resource availability and the size-dependence of resource acquisition. The size-dependence of P and ρ reflect the inherent size-limitations on cellular optical cross-section and diffusion of nutrients to the cell surface. Under many conditions, these rates will exceed the size-limitation on growth due to the metabolic network, so we emphasize that the expressions for P and ρ are potential resource acquisition rates, which may be limited by metabolic capacity M (Fig. 5).

Similar to the resource acquisition model, the size-scaling exponent of growth rate varies between $\frac{1}{3}$ and $\frac{3}{4}$ under various combinations of light and nutrient conditions (Fig. 6). When both NO_3^- and E are not limiting, growth is limited by a cell's metabolic capacity, with a size-scaling exponent of $\frac{3}{4}$. At constant, saturating irradiance, decreasing limiting NO_3^- reduces the size-scaling exponent of growth from $\frac{3}{4}$ to $\frac{1}{3}$, since growth is limited by diffusion of nutrients from bulk media to the cell surface, and diffusion is proportional to $V^{1/3}$. Under saturating NO_3^- concentrations, decreasing irradiance reduces the size-scaling exponent from $\frac{3}{4}$ to $\frac{2}{3}$, consistent with Finkel et al. (2004). These changes in size-scaling exponent of growth reflect the dynamic change in the degree of growth limitation by resource acquisition of NO_3^-, irradiance, and metabolic capacity. The modest qualitative differences in b_μ reported in Figs. 3 and 6 are a consequence of the different relative weights of the allometric factors determining growth rate. Changes in size-scaling exponent of cellular chlorophyll alter the allometric relationships of P and μ under light limitation (Fig. 7). Increasing the volume-scaling exponent of cellular chlorophyll from $\frac{2}{3}$ to 1, resulted in modest increases in the volume-scaling exponent of growth, μ, because of increased light acquisition by larger cells. The caveats from the resource acquisition model apply here, emphasizing the need to use a reasonable cellular chlorophyll volume-scaling exponent, most likely slightly larger than $\frac{2}{3}$.
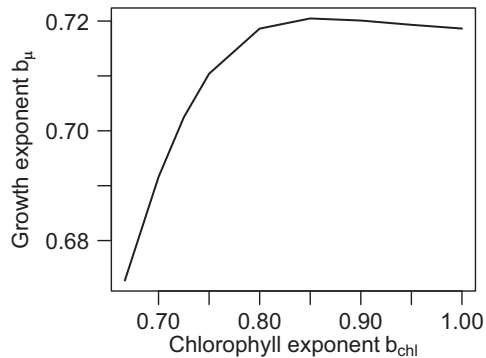

Fig. 4. Size-scaling exponent of growth rate as a function of the size-scaling exponent of cellular chlorophyll concentration under sufficient NO_3^- (100 μM) and limiting irradiance (20 μmol photons m^{-2} s^{-1}). Under saturating irradiance $b_\mu = \frac{3}{4}$.

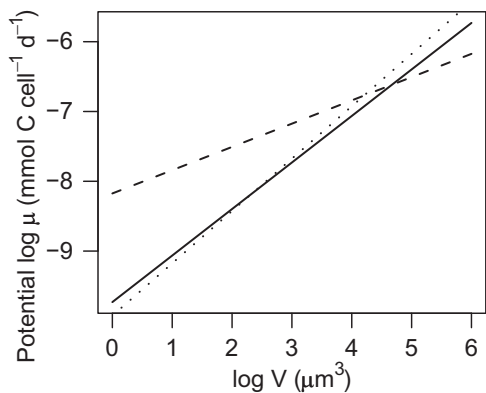**Fig. 5.** The allometric relationship of growth rate (μ, mmol C cell^{-1} d^{-1}) as computed from the minimum of photosynthesis at 100 μmol photons m^{-2} s^{-1} (P, solid line), nutrient uptake with NO_3^- concentration of 1 μM ($\frac{106}{16}\rho$, dashed line), and metabolic rates regulated by transportation networks (M, dotted line) from the metabolic transportation network model. Nutrient uptake has been converted to C units by multiplication by $\frac{106}{16}$.

4. Discussion

Incorporating phytoplankton community size structure will improve ocean models that aim to predict export production and trophic transfer to consumers (Baird and Suthers, 2007). The
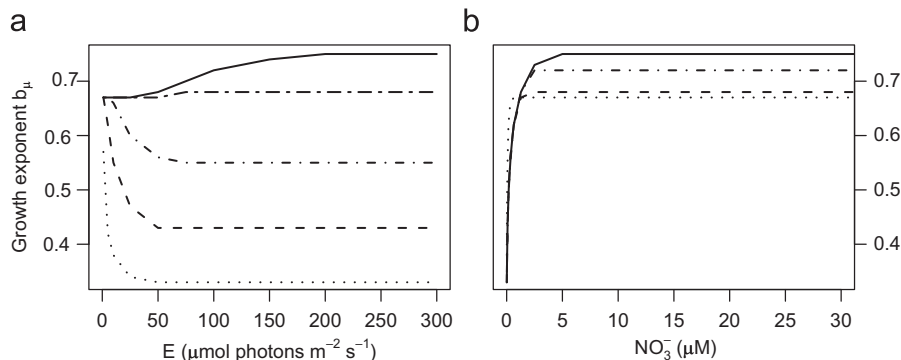

Fig. 6. The size-scaling exponents of growth rate, from the metabolic network model, (a) as a function of E (μmol photons m^{-2} s^{-1}) for NO_3^- concentration $= 0.01$ (dotted), 0.08 (dashed), 0.32 (dash–dotted), 1.3 (dash–long dash), 5 μM (solid), and (b) as a function of NO_3^- (μM) for $E = 10$ (dotted), 50 (dashed), 100 (dash–dotted), 250 μmol photons m^{-2} s^{-1} (solid). Cellular chlorophyll is $\propto V^{2/3}$.
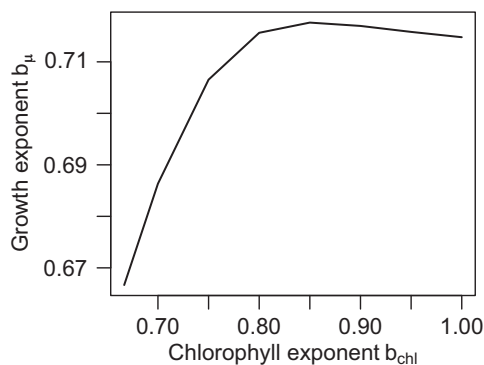
Fig. 7. Size-scaling exponent of growth rate as a function of the size-scaling exponent of cellular chlorophyll under limiting irradiance (25 µmol photons m^{-2} s^{-1}). Under saturating light $b_\mu = \frac{3}{4}$.

size-scaling of phytoplankton physiological rates are primary contributing factors to the size structure of phytoplankton communities (Irwin et al., 2006; Kriest and Oschlies, 2007). A detailed analysis of the relative importance of the size-scaling of these physiological processes over realistic ranges of resource availability will help with the parameterization of phytoplankton physiology in ecological and biogeochemical models. The $\frac{3}{4}$ rule of metabolic scaling predicts 10^6 fold variation in growth rate over the eight orders of magnitude of cell volume in phytoplankton, under resource saturated conditions. Any abiotic or biotic factor that alters the size-scaling of phytoplankton growth rate will alter the size structure of phytoplankton communities. Here we show how light and nutrient acquisition can interact with a size-dependent cellular metabolic transportation network to reduce the size-scaling exponent of growth from $\frac{3}{4}$ to $\frac{2}{3}$ or to as little as $\frac{1}{3}$ over realistic irradiance and nutrient regimes.

The size-scaling of maximum growth rates and the cellular metabolic network. Under optimal growth conditions, with light and nutrient concentration in excess of the requirements of growth, the transportation of resources throughout the metabolic network inside the cell constrains maximum growth rate $\propto V^{3/4}$ (mmol C cell^{-1} d^{-1}). If the allometry of the metabolic network is neglected then the size-scaling of maximum growth rate will depend on the size-scaling of maximum nutrient uptake and photosynthetic rates. Many models assume that the maximum nutrient uptake per cell is proportional to $V^{2/3}$ due to the change in surface area:volume with increasing cell size, therefore if nutrient acquisition limits growth, then maximum growth rate should be proportional to $V^{2/3}$. Alternatively, if carbon acquisition from photosynthesis controls growth rate then the size-scaling of the maximum photosynthetic capacity will set the size-scaling of maximum growth rate. If photosynthetic capacity is set by enzymatic reactions on the cell surface (inorganic carbon acquisition) then it may scale with $V^{2/3}$ but if as we propose in the resource acquisition model, it is set by the network of reactions (e.g., movement of resources from the acquisition of light energy, the electron transport chain and Calvin–Benson cycle), we expect P_{max} to scale with $V^{3/4}$. In the metabolic network model, we assume the metabolic transportation network regulates maximum resource acquisition rates and show that it provides a similar prediction to the resource acquisition model when $P_{max} \propto V^{3/4}$ and photosynthetic rate is assumed to be the ultimate control on maximum growth rate.

Cells of different sizes have different physiological responses to a particular set of resource conditions; large cells are more likely to find nutrient concentrations and light flux limiting than small cells. This is a consequence of differential allometries between maximum metabolic rates imposed by metabolic transportation

networks and the more severely limiting allometries of resource gathering processes; maximum growth rates $\propto V^{3/4}$, but under resource limiting conditions, growth rate will range from $V^{1/3}$ (for nutrients) to $V^{2/3}$ (for light). In its more severe form, nutrient limitation is determined by diffusion and will result in growth rates $\propto V^{1/3}$. Light limitation leads to size-scaling of photosynthetic rates roughly proportional to $V^{2/3}$ due to the geometric constraints on the absorption cross-section, with moderate deviations (to $V^{0.71}$, Figs. 4 and 7) due to size-dependent changes in intracellular chlorophyll concentration, pigment composition, photosynthetic architecture, distribution of plastids, and associated changes in the absorption efficiency per unit chlorophyll. Under intermediate concentrations of nutrient and photon flux densities the growth rate for larger cells can be resource limited while smaller cells are resource saturated within the same community, causing size-scaling exponents for growth intermediate between those set by extreme light or nutrient limitation. This occurs because larger cells have lower rates of nutrient diffusion and light absorption per unit volume and larger resource requirements for positive growth.

Our models suggest that variable resource conditions could be responsible for the variability in size-scaling exponents of growth (Schlesinger et al., 1981; Sommer, 1989; Finkel, 2001) and biomass (Peters, 1983b; Sprules and Munawar, 1986; Cavender-Bares et al., 2001; Belgrano et al., 2002; Finkel et al., 2009) reported in a wide range of field and laboratory studies. Interpreting observations of the size-scaling of phytoplankton community biomass and productivity rates in field studies can be challenging. As resource availability changes, the observer may note the loss of a size class, which may affect the interpretation of size-scaling exponents. As abundances decrease, the size of sample necessary to observe large cells increases quite rapidly because of the power-law decrease in abundance and rates (Sheldon and Kerr, 1972; Belgrano et al., 2002). If an narrow range of cell sizes is being measured, perhaps only picoplankton or only nannoplankton, the observer may see changes in abundance or loss of size class that swamps the ability to detect changes in size-scaling exponents. Finally, we note that across broad taxonomic groups, intercepts on size-scaling growth relationships may change, resulting in complex patterns that alter the patterns discussed here, which we developed for a single taxonomic class. Multiple taxonomic groups can be incorporated in our framework by allowing for different metabolic rates independent of size, i.e., the intercepts in Table 1 (Moloney and Field, 1989; Raven et al., 2005; Irwin et al., 2006). Many additional factors must be considered to predict net community growth rates and size structure, such as loss processes, including sinking, grazing, and viral attack, and can be added to our framework. Temperature dependence of metabolic rates can be incorporated with an Arrhenius factor in the intercept of the growth allometry (Gillooly et al., 2001) and by introducing the temperature dependence of the diffusion constant.

5. Conclusion

Ocean models predict phytoplankton community structure by predicting growth as a function of irradiance and nutrient concentration. Many ecological and biogeochemical processes are now being described using phytoplankton community size structure. In order to predict the size-structure of phytoplankton communities, we need to know how cell size interacts with light and nutrient acquisition to alter growth rates. We have shown how to describe the size dependence of growth due to an interaction between the allometry of resource acquisition and metabolic constraints imposed by a metabolic transportation

network. We predict a size-scaling exponent of resource saturated growth of $\frac{3}{4}$ with smaller exponents as low as $\frac{2}{3}$ and $\frac{1}{3}$ for light-limited and nutrient-limited growth, respectively. Additional data are needed to confirm the predicted relationships as a function of limiting resources. We have used cell volume as the measure of cell size because biophysical processes that regulate resource acquisition depend on cell volume. Phytoplankton biomass may increase less than linearly with volume, possibly proportional to $V^{3/4}$, which may alter the metabolic transportation network effect on growth allometry. Additionally, cellular carbon and nitrogen (known as quotas) vary with resource conditions and allometrically. An extension of this model which permits dynamic cell quotas should be developed to predict growth rates in environments with varying resource availabilities.

Acknowledgments

References

Agustí, S., 1991. Allometric scaling of light absorption and scattering by phytoplankton cells. Canadian Journal of Fisheries and Aquatic Sciences 48, 763–767.

Aksnes, D.L., Egge, J.K., 1991. A theoretical model for nutrient uptake in phytoplankton. Marine Ecology Progress Series 70, 65–72.

Armstrong, R.A., 2003. A hybrid spectral representation of phytoplankton growth and zooplankton response: the "control rod" model of plankton interaction. Deep Sea Research II 50, 2895–2916.

Armstrong, R.A., 2008. Nutrient uptake rates as a function of cell size and surface transporter density: a Michaelis-like approximation to the model of Pasciak and Gavis. Deep-Sea Research I 55, 1311–1317.

Baird, M.E., Suthers, I.M., 2007. A size-resolved pelagic ecosystem model. Ecological Modelling 203, 185–203.

Banavar, J.R., Damuth, J., Maritan, A., Rinaldo, A., 2002. Supply-demand balance and metabolic scaling. Proceedings of the National Academy of Sciences of the United States of America 99, 10506–10509.

Belgrano, A., Allen, A.P., Enquist, B.J., Gillooly, J.F., 2002. Allometric scaling of maximum population density: a common rule for marine phytoplankton and terrestrial plants. Ecology Letters 5, 611–613.

Berg, H.C., Purcell, E.M., 1977. Physics of chemoreception. Biophysical Journal 20, 193–219.

Cavender-Bares, K.K., Rinaldo, A., Chisholm, S.W., 2001. Microbial size spectra from natural and nutrient enriched ecosystems. Limnology and Oceanography 46 (4), 778–789.

Cermeño, P., Marañón, E., Harbour, D., Harris, R.P., 2006. Invariant scaling of phytoplankton abundance and cell size in contrasting marine environments. Ecology Letters 9, 1210–1215.

Chisholm, S.W., 1992. Phytoplankton size. In: Primary Productivity and Biogeochemical Cycles in the Sea. Plenum Press, New York, pp. 213–237.

Dodds, P.S., Rothman, D.H., Weitz, J.S., 2001. Reexamination of the '3/4 laws' of metabolism. Journal of Theoretical Biology 209, 9–27.

Falkowski, P.G., 1991. Species variability in the fractionation of ^{13}C and ^{12}C by marine phytoplankton. Journal of Plankton Research 13 (Suppl.), 21–28.

Falkowski, P.G., Raven, J.A., 2007. Aquatic Photosynthesis, second ed. Princeton University Press, Princeton, NJ.

Finkel, Z.V., 2001. Light absorption and size scaling of light-limited metabolism in marine diatoms. Limnology and Oceanography 46 (1), 86–94.

Finkel, Z.V., Irwin, A.J., Schofield, O., 2004. Resource limitation alters the 3/4 size scaling of metabolic rates in phytoplankton. Marine Ecology-Progress Series 273, 269–279.

Finkel, Z.V., Jacob-Vaillancourt, C., Irwin, A.J., Reavie, E.D., Smol, J.P., 2009. Environmental control of diatom community size structure varies across aquatic ecosystems. Proceedings of the Royal Society B 276, 1627–1634.

Finkel, Z.V., Katz, M.E., Wright, J.D., Schofield, O.M.E., Falkowski, P.G., 2005. Climatically driven macroevolutionary patterns in the size of marine diatoms over the cenozoic. Proceedings of the National Academy of Sciences of the United States of America 102 (25), 8927–8932.

Finkel, Z.V., Sebbo, J., Feist-Burkhardt, S., Irwin, A.J., Katz, M.E., Schofield, O.M.E., Young, J.R., Falkowski, P.G., 2007. A universal driver of macroevolutionary change in the size of marine phytoplankton over the cenozoic. Proceedings of the National Academy of Sciences of the United States of America 104 (51), 20416–20420.

Fujiki, T., Taguchi, S., 2002. Variability in chlorophyll a specific absorption coefficient in marine phytoplankton as a function of cell size and irradiance. Journal of Plankton Research 24 (9), 859–874.

Gillooly, J.F., Brown, J.H., West, G.B., Savage, V.M., Charnov, E.L., 2001. Effects of size and temperature on metabolic rate. Science 293 (5538), 2248–2251, 475AL SCIENCE.

Grover, J.P., 1991. Resource competition in a variable environment: phytoplankton growing according to the variable internal-stores model. American Naturalist 138, 811–835.

Harrison, W.G., Harris, L.R., Irwin, B.D., 1996. The kinetics of nitrogen utilization in the oceanic mixed layer: nitrate and ammonium interactions at nanomolar concentrations. Limnology and Oceanography 41, 16–32.

Hemmingsen, A.M., 1960. Energy metabolism as related to body size and respiratory surfaces, and its evolution. Reports of the Steno Memorial Hospital 9 (2), 15–22.

Irwin, A.J., Finkel, Z.V., Schofield, O.M.E., Falkowski, P.G., 2006. Scaling-up from nutrient physiology to the size-structure of phytoplankton communities. Journal of Plankton Research 28 (5), 459–471.

Kiørboe, T., 1993. Turbulence, phytoplankton cell size, and the structure of pelagic food webs. Advances in Marine Biology 29, 1–72.

Kleiber, M., 1947. Body size and metabolic rate. Physiological Reviews 27, 511–541.

Kriest, I., Oschlies, A., 2007. Modelling the effect of cell-size-dependent nutrient uptake and exudation on phytoplankton size spectra. Deep-Sea Research I 54, 1593–1618.

Laws, E.A., Falkowski, P.G., Smith, W.O., Ducklow, H., McCarthy, J.J., 2000. Temperature effects on export production in the open ocean. Global Biogeochemical Cycles 14, 1231–1246.

Li, W.K.W., 2002. Macroecological patterns of phytoplankton in the northwestern North Atlantic ocean. Nature 419, 154–157.

López-Urrutia, A., San Martin, E., Harris, R.P., Irigoien, X., 2006. Scaling the metabolic balance of the oceans. Proceedings of the National Academy of Sciences of the United States of America 103, 8739–8744.

MacIntyre, H.L., Kana, T.M., Anning, J., Geider, R., 2002. Photoacclimation of photosynthesis irradiance response curves and photosynthetic pigments in microalgae and cyanobacteria. Journal of Phycology 38, 17–38.

Menden-Deuer, S., Lessard, E., 2000. Carbon to volume relationships for dinoflagellates, diatoms, and other protist plankton. Limnology and Oceanography 45, 569–579.

Moloney, C.L., Field, J.G., 1989. General allometric equations for rates of nutrient uptake, ingestion, and respiration in plankton organisms. Limnology and Oceanography 34 (7), 1290–1299.

Morel, A., Bricaud, A., 1981. Theoretical results concerning light absorption in a discrete medium, and application to specific absorption of phytoplankton. Deep-Sea Research I 28A, 1375–1393.

Munk, W.H., Riley, G.A., 1952. Absorption of nutrients by aquatic plants. Journal of Marine Research 11 (2), 215–240.

Pasciak, W.J., Gavis, J., 1974. Transport limitation of nutrient uptake in phytoplankton. Limnology and Oceanography 19, 881–888.

Pasciak, W.J., Gavis, J., 1975. Transport limited nutrient uptake rates in *Ditylum brightwellii*. Limnology and Oceanography 20, 604–617.

Peters, R.H., 1983a. The Ecological Implications of Body Size. Cambridge University Press, Cambridge.

Peters, R.H., 1983b. Size structure of the plankton community along the trophic gradient of lake Memphremagog. Canadian Journal of Fisheries and Aquatic Sciences 40, 1770–1778.

Raven, J.A., Finkel, Z.V., Irwin, A.J., 2005. Picophytoplankton: bottom-up and top-down controls on ecology and evolution. Vie at Milieu 55, 209–215.

Raven, J.A., Waite, A.M., 2004. The evolution of silicification in diatoms: inescapable sinking and sinking as escape? New Phytologist 162 (1), 45–61.

Richardson, K., Beardall, J., Raven, J.A., 1983. Adaptation of unicellular algae to irradiance: an analysis of strategies. New Phytologist 93, 157–191.

Schlesinger, D.A., Molot, L.A., Shuter, B.J., 1981. Specific growth rates of freshwater algae in relation to cell size and light intensity. Canadian Journal of Fisheries and Aquatic Science 38, 1052–1058.

Sheldon, R.W., Kerr, S.R., 1972. The population density of monsters in Loch Ness. Limnology and Oceanography 17 (5), 796–798.

Sicko-Goad, L.M., Schekske, C.L., Stoermer, E.F., 1984. Estimation of intracellular carbon and silica content of diatoms from natural assemblages using morphometric techniques. Limnology and Oceanography 29 (6), 1170–1178.

Sommer, U., 1989. Maximal growth rates of Antarctic phytoplankton: only weak dependence on cell size. Limnology and Oceanography 34 (6), 1109–1112.

Sprules, W.G., Munawar, M., 1986. Plankton size spectra in relation to ecosystem productivity, size and perturbation. Canadian Journal of Fisheries and Aquatic Sciences 43, 1789–1794.

Strathmann, R.R., 1967. Estimating the organic carbon content of phytoplankton from cell volume or plasma volume. Limnology Oceanography 12, 411–418.

Tremblay, J.-E., Klein, B., Legendre, L., Rivkin, R.B., Therriault, J.-C., 1997. Estimation of f-ratios in ocean based on phytoplankton size structure. Limnology and Oceanography 42, 595–601.

Verity, P.G., Robertson, C.Y., Tronzo, C.R., Andrews, M.G., Nelson, J.R., Sieracki, M.E., 1992. Relationships between cell volume and the carbon and nitrogen content of marine photosynthetic nanoplankton. Limnology and Oceanography 37, 1434–1446.

West, G.B., Brown, J.H., Enquist, B.J., 1997. A general model for the origin of allometric scaling laws in biology. Science 276, 122–126.